Hybrid Power/Energy Generation Through Multidisciplinary and Multilevel Design Optimization With Complementarity Constraints

Shen Lu
e-mail: shenlu2@illinois.edu

Nathan B. Schroeder
e-mail: nschroe2@illinois.edu

Harrison M. Kim[1]
e-mail: hmkim@illinois.edu

Uday V. Shanbhag
e-mail: udaybag@illinois.edu

Department of Industrial and Enterprise Systems Engineering,
University of Illinois at Urbana-Champaign,
Urbana, IL 61801

The optimal design of hybrid power generation systems (HPGSs) can significantly improve the technical and economic performance of power supply. However, the discrete-time simulation with logical disjunctions involved in HPGS design usually leads to a nonsmooth optimization model, to which well-established techniques for smooth nonlinear optimization cannot be directly applied. This paper casts the HPGS design optimization problem as a multidisciplinary design optimization problem with complementarity constraints, a formulation that introduces a complementarity formulation of the nonsmooth logical disjunction, as well as a time horizon decomposition framework, to ensure a fast local solution. A numerical study of a stand-alone hybrid photovoltaic/wind power generation system is presented to demonstrate the effectiveness of the proposed approach. [DOI: 10.1115/1.4002292]

1 Introduction

In many regions of the world, the topography of the landscape prevents connectivity to the electrical grid. In these cases, one no longer has access to the grid and the traditional power source has been a diesel generator. However, the rising cost of fuel and the associated fuel transportation costs are making this option less desirable. In addition to the recurring costs accompanying diesel generation, the quantification of the environmental impact due to emissions is of increasing concern [1]. One alternative that bypasses these issues associated with diesel power is distributed generation using renewable resources.

Distributed power generation using renewable energy sources presents a promising alternative due to cost and environmental concerns [1]. As renewable energy sources are extremely variable and unpredictable by nature, they are usually combined with battery storage to ensure reliability, leading to a hybrid power generation system (HPGS) [2]. Currently, energy conversion techniques using renewable resources such as wind and solar have been developed to the point where a HPGS consisting of these two components and an energy storage method is price competitive with a grid extension in some locations. As the price of HPGS is reduced further, they will soon become competitive with grid power [1].

1.1 Hybrid Power Generation System Design. The design decision at the system level (e.g., system sizing, configuration, and operation) has been identified as a key driver of HPGS cost reduction and plays an increasingly important role in HPGS design. Current HPGSs are often overbuilt in order to ensure that power is supplied even if the available resources are performing well below average. If an optimal design can be determined for a given location, the components with the minimal, while adequate, capacity can be employed, significantly reducing the system cost.

Many efforts have been made to facilitate the effective design of HPGSs: Individual components have been captured with mathematical models at various fidelities (refer to Sec. 2), and system performances (i.e., the HPGS's ability to supply the load) have been estimated either through chronological simulations based on resource data or through probabilistic techniques that account for the resource fluctuations [2]. In addition, optimization procedures have been used to derive optimal HPGSs for given situations. Methods currently in use include graphic construction methods [3], probabilistic approaches [4], enumerative approaches [5], and artificial intelligence methods [6,1]. Some of these methods, such as graphic construction methods and enumerative approaches, involve procedures that lack autonomous design, while the other methods, such as probabilistic approaches and artificial intelligence methods, either incur intensive computation or suffer from suboptimal solutions.

The design optimization of HPGSs involves discrete-time simulation of the system over a certain time period. This setting presents two challenges for numerical optimization. First, the dynamics of such systems is usually discrete in nature. The systems include nonsmooth logical disjunctions, e.g., switching between different sets of equations based on working conditions, and other nonsmooth functions, such as minimum and maximum operations. Due to this discrete nature, well-established optimization techniques for smooth problems cannot be applied to such systems. Second, the consideration of system performance at each time step introduces additional variables (referred to as time dependent variables) to the optimization model, thus increasing the size of the problem. As the number of time steps increases, solving the HPGS design optimization problem with an all-in-one (AIO) approach, which handles all the variables in a single optimization problem, may become impractical, undesirable, or even impossible.

Traditionally, one way of capturing logical disjunctions is to introduce discrete variables. However, such a mixed integer optimization model usually incurs intensive computational cost for large problems as the worst case solution time grows exponentially with the number of discrete variables. Alternatively, heuristic schemes such as genetic algorithm can be integrated with the discrete-time simulation. While this type of approach is robust, in general, it also suffers from the lack of guarantees for optimality. In this paper, a different track of handling the discreteness is pre-

[1]Corresponding author.

Contributed by the Design Automation Committee of ASME for publication in the JOURNAL OF MECHANICAL DESIGN. Manuscript received December 11, 2008; final manuscript received July 21, 2010; published online October 4, 2010. Assoc. Editor: Timothy W. Simpson.

sented through the aid of complementarity constraints (CCs). Complementarity is a relationship between functions (variables) where either one (or both) must be at its boundary. An example of the CC is given as follows:

$$\mathbf{0} \leq \mathbf{F}(\mathbf{x}) \perp \mathbf{G}(\mathbf{x}) \geq \mathbf{0} \tag{1}$$

where $\mathbf{x}$ represents the variables and $\mathbf{F}$ and $\mathbf{G}$ are multifunctions in $\mathbf{R}^p$. Particularly, the symbol $\perp$ indicates that $\mathbf{G}$ and $\mathbf{F}$ are nonnegative and that either $[\mathbf{G}]_j$ or $[\mathbf{F}]_j$ or both are zero for $j=1,\ldots,p$. The CC in Eq. (1) can be equivalently converted into the following set of inequality constraints:

$$\mathbf{F} \geq \mathbf{0}, \quad \mathbf{G} \geq \mathbf{0}, \quad \mathbf{G}(\mathbf{x}) \circ \mathbf{F}(\mathbf{x}) \leq \mathbf{0} \tag{2}$$

where the symbol $\circ$ represents the Hadamard product, i.e., the term-by-term product operation between two vectors: $\mathbf{a} \circ \mathbf{b} = [a_1,\ldots,a_n]^T \circ [b_1,\ldots,b_n]^T = [a_1 b_1,\ldots,a_n b_n]^T$.

CCs can arise from various physical, economic, and procedural considerations of engineering applications. The readers are referred to Ref. [7] for a brief discussion on the relevance of CCs to multidisciplinary design. In particular, CCs are useful in HPGS design optimization, as discussed in Sec. 3, in that they can be used to model certain types of logical disjunctions in discrete-time system models without the use of binary variables. Since general approaches for mixed integer optimization usually incur intensive computation cost for a large problem with many discrete variables, the CC offers an alternative for some classes of disjunctive problems and can be embedded within a standard nonlinear programming (NLP) solver to obtain fast local solutions. In addition, a certain level of local optimality can be ensured from this approach, supported by established theories in mathematical programs with complementarity constraints (MPCCs).

In order to handle the size issue of HPGS design optimization, various decomposition-based approaches [8] can be applied so that the AIO problem can be solved through an iterative solution of smaller, inter-related subproblems and coordination among them. In this paper, we utilize the repetition of the simulation and decision making of HPGS at individual time steps and present a time horizon decomposition framework, which decomposes the AIO HPGS design optimization problem into a set of consecutive stage optimization subproblems.

1.2 MDO and Mathematical Programs With Complementarity Constraints. Multidisciplinary design optimization [9] (MDO) has been investigated extensively over the past decades. MDO problems can be solved directly with so-called AIO approaches, which handle all the variables in a single optimization problem. The implementation of the AIO approach is straightforward; however, it may become impractical as the complexity of the problem increases. As an alternative to the AIO approaches, several MDO methods are currently available. These methods include concurrent subspace optimization [10], bilevel integrated system synthesis [11], collaborative optimization (CO) [12], the constraint margin approach [13], analytical target cascading (ATC) [14], penalty decomposition (PD) [15], and augmented Lagrangian decomposition (ALD) [16]. Solving MDO problems with decomposition approaches could be advantageous for many reasons. Computationally, it breaks the AIO problems into smaller subproblems usually easier to solve; it also allows specialized algorithms to be applied to each subproblem. Organizationally, it keeps the individual disciplinary design optimizations as independent as possible with a minimum amount of communication, making it possible to integrate existing disciplinary analysis codes at small expense.

Among all the variants of MDO, the quasi-separable MDO problem has gained particular attention during recent years. Many of the above mentioned MDO methods (e.g., CO, constraint margin approach, PD, and ALD) can be considered as the quasi-separable MDO problem. In addition to these, Ref. [17] proposed an ATC variant with local objectives under the context of multimode design optimization. Among these approaches, PD, ATC, and ALD have been shown to have formulations whose solutions satisfy the Karush–Kuhn–Tucker (KKT) conditions of the original problems under certain assumptions.

MPCCs represent an active research area that is not well connected to the MDO. In order to solve an MPCC, one intuitive approach is to reformulate it into a nonlinear programming problem through replacing the CCs (Eq. (1)) with its equivalent inequality constraints (Eq. (2)). However, the resulting nonlinear program usually fails to satisfy the linear independence constraint qualification (LICQ) [18] and the weaker Mangasarian–Fromovitz constraint qualification (MFCQ) [18] at every feasible point. The failure of these constraint qualifications may have important implications: The multiplier set may be unbounded; the active constraint normals may be linearly dependent; and a linear relaxation of the reformulated nonlinear programming problem can become inconsistent arbitrarily close to a solution of the MPCC [19]. As a consequence, existing nonlinear programming techniques may have difficulties solving this type of problem.

Significant efforts have been made to investigate the MPCC solution algorithm over the past few years. Reference [19] followed the reformulation approach and reported promising results using sequential quadratic programming (SQP) methods. Reference [20] provided global convergence theory for SQP methods. Some other methods solve a sequence of nonlinear programs with penalized CCs [21,22]. An important class of methods, known as regularization methods, requires the solution of a sequence of regularized problems involving the relaxed constraints $\mathbf{G}(\mathbf{x},\mathbf{y}) \circ \mathbf{F}(\mathbf{x},\mathbf{y}) \leq \mathbf{t}_k$, with $\mathbf{t}_k \to 0$. These regularized problems may be solved by interior methods or by SQP methods. Along this line of research, Refs. [23–25] presented interior methods under various assumptions; Ref. [26] proposed an interior point method that converges to a second-order KKT point and extended this method to stochastic MPCC using scenario-based decomposition; Ref. [27] discussed a two-sided relaxation scheme and provided local convergence theory for an interior method coupled with such a relaxation scheme.

MDO problems with complementarity constraints (MDO-CC) are not frequently addressed in existing literature. In Ref. [28], the authors recently presented an augmented Lagrangian decomposition formulation for this problem to show the equivalence between the AIO formulation and the decomposed formulation. Reference [7] proposed a regularized inexact penalty decomposition (RIPD) algorithm for MDO-CC and established the convergence properties of the RIPD algorithm. Additionally, Ref. [26] presented a scenario-based decomposition formulation for stochastic MPCCs and then solved it as an AIO problem with a parallel algorithm.

In this paper, we present a mathematical model of HPGS design for cost minimization under the zero loss of power supply constraint. In addition, a multidisciplinary design optimization problem with complementarity constraint approach is presented, which first reformulates the logical disjunction in the HPGS simulation into CCs and then solves the reformulated problem with a multidisciplinary decomposition framework. The proposed algorithm is tested with a HPGS design case study at Corsica Island in France, and the numerical results are encouraging.

The paper is organized as follows: In Sec. 2, the HPGS design problem is stated, with component and system models described. In Sec. 3, the complementarity reformulation of the HPGS design problem is presented, followed by its multidisciplinary decomposed formulation. In addition, the correspondence between the stationarity conditions of the complementarity formulation and those of the decomposed formulation is established, and an augmented Lagrangian decomposition algorithm is presented based on the correspondence. A numerical study of an HPGS design case is presented in Sec. 4, and conclusions are drawn in Sec. 5.

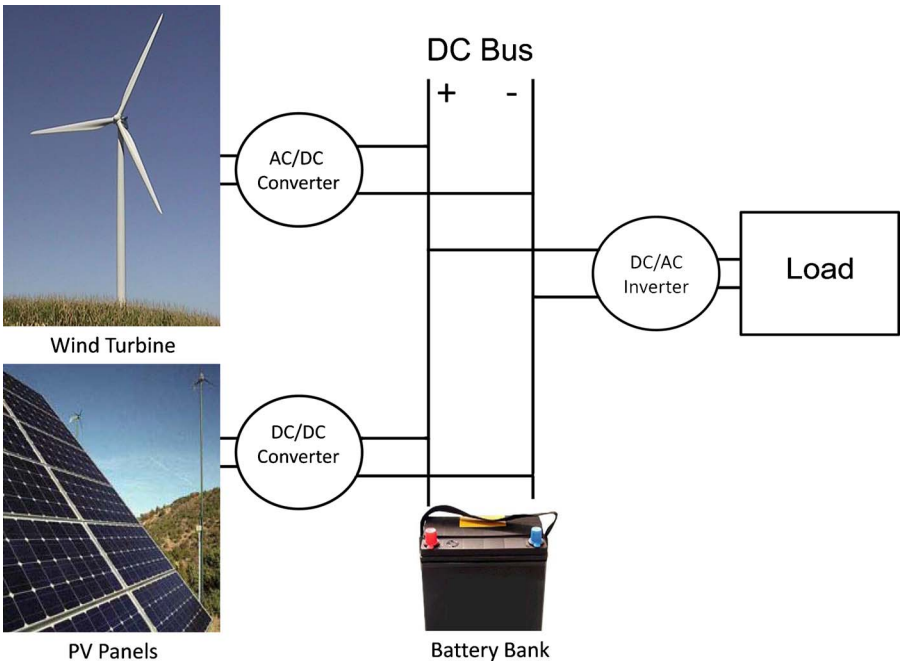

Fig. 1 Schematic of hybrid power generation system

2 Hybrid Power Generation System Design

In this section, the HPGS will be described in detail. The system configuration will be specified, the individual component models will be shown, and the cost calculation will be explained.

2.1 System Configuration. HPGSs can be assembled in a variety of ways. Some models include diesel generators as back-up power [29], while others rely solely on battery back-up. The components can also be connected in different manners. In the case of a high wind potential site, for example, it may be prudent to feed the ac energy produced by the wind turbine directly to the load via an uninterruptible power supply [30]. This would allow for bypassing the battery and related converters to increase efficiency.

The power system in consideration here is a stand-alone hybrid photovoltaic (PV)/wind system at a remote location. This system consists of a PV generator, a wind generator, and a battery storage device, which are connected to a dc bus through the proper converters. In addition, the energy generated by, or stored in, the system is contributed to a remote load through a dc/ac inverter with enough capacity to meet the peak load demand. Figure 1 shows the configuration of the HPGS in consideration.

2.2 Component Models. The mathematical models of the three principal components, the PV generator, the wind generator, and the battery storage, are presented in this subsection.

2.2.1 Mathematical Model of PV Generator. PV panels are affected by many factors in very complex ways. Extremely accurate models can include up to eight variables [31]. In order to bypass some of this complexity, engineering applications regarding PV panels often use simplified simulation models, which typically include the power efficiency models [2]. Here, a simplified mathematical model is employed to estimate the power output (p_{PV}) in terms of watt-hour of the PV generator:

$$p_{\mathrm{PV}}(t) = \eta_{\mathrm{PV}} \cdot G_{\beta}(t) \cdot a_{\mathrm{PV}} \tag{3}$$

In this model, G_{β} is the solar irradiance in $\mathrm{W/m^2}$, η_{PV} is the efficiency of the solar panels in converting the solar energy into electricity, and a_{PV} is the area of the panels in $\mathrm{m^2}$ for a given iteration.

2.2.2 Mathematical Model of Wind Turbine. Though fewer variables are needed to describe wind generators, modeling a range of sizes poses its own challenge. This is because wind generators have their own unique power curves relating the current wind speed to the energy produced. Because the wind generator to be installed in the system is an output of the design process and therefore unknown during the design phase, a power curve unique to a specific make and model will not suffice. Instead, a generic model must be used to cover a wide range of wind generator sizes. This is typically done by relating the wind speed to the average power using either a piecewise function, a Weibull parameter, or quadratic expressions [2,32].

The model used here considers a piecewise output function of the wind generator (p_w) given the cut-in wind speed (V_{in}), cut-out wind speed (V_{out}), rated wind speed (V_r), and actual environmental wind speed (v). All these speeds are measured in $\frac{m}{s}$ and are used to determine the power generated as follows:

$$p_w(t) = \begin{cases} p_r(v^2 - V_{\mathrm{in}}^2/V_r^2 - V_{\mathrm{in}}^2), & V_{\mathrm{in}} \le v \le V_r \\ p_r, & V_r \le v \le V_{\mathrm{out}} \\ 0, & v \le V_{\mathrm{in}} \text{ or } v \ge V_{\mathrm{out}} \end{cases} \tag{4}$$

As each wind turbine has its own design objectives, there will be varying V_{in}, V_{out}, and V_r values. The proper wind turbine dynamics can be determined in the same manner as stand-alone wind turbines, with the goal of matching the characteristic velocities to the location's resources in order to maximize power production [33].

2.2.3 Mathematical Model of Battery. As batteries are chemically and physically complex, so are the models used to predict their behavior [34]. In the design of a HPGS, the battery is addressed in terms of energy storage and throughput. Therefore, the internal processes of the battery are immaterial, and the battery model needs only to reflect the energy losses inflicted by the battery. This is done by using an efficiency parameter determined to represent the average loss of energy in a battery system [30,35].

Here, we employ an approximated battery model considering the state of charge of the battery. The model used requires only the nominal capacity (c_{nbat}) and the charging efficiency (η_{ch}) of the

batteries as inputs and assumes that the efficiency is independent of the current state of charge. As there are maximum and minimum levels of possible energy storage for any battery system, these limits need to be accounted for in the model:

$$C_{\text{bat min}} = c_{\text{nbat}} \cdot \text{DoD}$$

$$C_{\text{bat max}} = c_{\text{nbat}} \tag{5}$$

where DoD represents the depth of discharge of the battery (the percentage of energy that can be drained from the battery without damaging it). As the model progresses to subsequent time steps, the state of charge needs to be updated based on the power generated and consumed during the previous step, subject to $C_{\text{bat min}}$ and $C_{\text{bat max}}$. If the power generated is greater than the load during a given time step, then the excess electricity is stored in the battery according to the following equation:

$$c^*_{\text{bat}}(t) = c_{\text{bat}}(t-1) + \left(p_{\text{PV}}(t)\,\eta_{\text{PV}} + p_w(t)\,\eta_w - \frac{p_{\text{load}}(t)}{\eta_l} \right) \eta_{\text{ch}}$$

$$c_{\text{bat}}(t) = \min\{c^*_{\text{bat}}(t), C_{\text{bat max}}\} \tag{6}$$

where $c_{\text{bat}}(t)$ is the state of charge of the battery at the end of time step t, $c^*_{\text{bat}}(t)$ is an intermediate variable, $p_{\text{PV}}(t)$ is the power produced by the PV module during time step t, $p_w(t)$ is the power produced by the wind turbine during time step t, and $p_{\text{load}}(t)$ is the power required by the load during time step t. In addition to the power generated and that required by the load, there are also losses associated with the power converters in the system. This model uses a central dc bus connected to the battery terminals, and each element (PV, wind turbine, and load) is connected to this bus via a power converter. η_{PV} is the efficiency coefficient of the dc/dc converter connecting the PV panels, η_w represents the ac/dc for the wind turbine, and η_l represents the dc/ac inverter connected to the load. If the power generated is less than the load requirement, the battery is used to satisfy the remaining load and is updated as follows:

$$c^*_{\text{bat}}(t) = c_{\text{bat}}(t-1) + \left(p_{\text{PV}}(t)\,\eta_{\text{PV}} + p_w(t)\,\eta_w - \frac{p_{\text{load}}(t)}{\eta_l} \right) \eta_{\text{dis}}$$

$$c_{\text{bat}}(t) = \max\{c^*_{\text{bat}}(t), C_{\text{bat min}}\} \tag{7}$$

The only difference between the charging and discharging cases is the efficiency coefficient. In a physical battery, there would be energy lost from various causes. However, this model lumps all energy losses in the battery and considers them only while charging. Since all losses are considered while the battery is charging, the discharge efficiency is set to be 100%. It has been found that a range of 65–85% is an appropriate efficiency value for battery throughput [35].

We note that the battery operation includes an if statement, and hence a logical disjunction, in its expression. As discussed in Sec. 1, this logical disjunction leads to a nonsmooth optimization model, presenting a challenge to HPGS design optimization. The matter will be addressed in Sec. 3.

2.3 Overall System Optimization Model. In this subsection, we present a HPGS design optimization problem, which determines the capacity of the three principal components of the system, i.e., a_{PV}, p_w, and c_{nbat}. In the selection of the optimal system capacity, the cost of the system must typically be balanced by the reliability of the provided power. In this model, the load is assumed to be sensitive and thus cannot afford any loss of power supply. Accordingly, the reliability of the system does not need to be penalized as any system resulting in a time step of unsatisfied load is treated as infeasible. Therefore, the system can be optimized with respect to cost only.

2.3.1 Cost Objective Function. There are many metrics for measuring the cost of a HPGS. These include the net present cost, the levelized cost of energy (LCE), and the life-cycle cost [2]. Of these three metrics, the LCE has an advantage in terms of units. The LCE is measured in \$/kW h, which is a unit that allows a comparison between the HPGS and other sources of power. The other metrics, net present cost and life-cycle cost, are measured in terms of \$, which does not allow for a direct comparison with grid-based power. Because of this advantage, the LCE will be used in this case study.

In determining the cost of a HPGS, many factors need to be accounted for. Each component has an initial cost and some form of maintenance and operational costs, and it could need replacement before the intended lifetime of the system has passed. Though all power converters are considered individually with regard to their efficiency, the converters connected to components are treated as a subunit of that component for the calculation of costs. This means that the wind generator contains its ac/dc converter and that the PV panels are purchased with their dc/dc converters included in the price. They are also assumed to have the same expected lifetime, which means that the combination of component and converter can be considered as one in the cost calculation. However, this simplification does not apply to the dc/ac inverter needed to supply the load as it is an independent component. As such, the inverter's costs must also be added to the system, as with the costs of the battery, wind generator, and PV panels.

2.3.1.1 Initial cost. The initial costs (C_{init}) of the components must include not only the parts costs, but also the installation cost. To account for this installation fee, a percentage of the purchase price of the components is added to the initial costs (represented as 1.2, i.e., 20%) [30]. To calculate the initial cost of a component, the size (S_{comp}) must be multiplied by the unit cost of the component (C_{unit}). As an example, for the wind generator, C_{unit} has units of \$/W, and S_{comp} is in watts,

$$C^{\text{wind}}_{\text{init}} = 1.2 S^{\text{wind}}_{\text{comp}} \cdot C^{\text{wind}}_{\text{unit}} \tag{8}$$

2.3.1.2 O&M cost. Because fuel is not used in any component of the HPGS, the only annually recurring cost is the operation and maintenance (O&M) cost (C_{om}). This is calculated as a percentage of the initial cost. As O&M costs are annual costs, the percentage must be multiplied by the project lifetime (T) and the initial cost to determine the total O&M cost for a component. Again, taking the wind generator with a 3% O&M, for example, the O&M cost is calculated as

$$C^{\text{wind}}_{\text{om}} = 0.03 C^{\text{wind}}_{\text{init}} T \tag{9}$$

2.3.1.3 Replacement cost. Not all components of a HPGS have expected lifetimes that will meet or exceed the project lifetime. In order to accurately account for this fact, components will need to be replaced at the end of their respective lifetimes until the project has reached completion. The PV panels typically will have the longest life and thus will set T. Other components that will deteriorate before then need to be replaced. This replacement cost (C_{rep}) is calculated as follows [36]:

$$C_{\text{rep}} = C_{\text{unit}} \cdot S_{\text{comp}} \sum_{i=1}^{\frac{T}{L_{\text{comp}}}} \left(\frac{1+g}{1+d} \right)^{i * L_{\text{comp}}} \tag{10}$$

where L_{comp} is the useful lifetime of the component in years, g is the inflation rate of component replacements, and d is the discount rate.

2.3.1.4 Cost calculation. To combine the costs mentioned above, the variable C_{tot} is introduced. C_{tot} is the summation of the three aforementioned costs for each component in the system: wind, PV, battery, and inverter,

$$C_{\text{tot}} = C_{\text{init}}^{\text{wind}} + C_{\text{om}}^{\text{wind}} + C_{\text{rep}}^{\text{wind}} + C_{\text{init}}^{\text{PV}} + C_{\text{om}}^{\text{PV}} + C_{\text{init}}^{\text{bat}} + C_{\text{om}}^{\text{bat}} + C_{\text{rep}}^{\text{bat}} + C_{\text{init}}^{\text{inv}} + C_{\text{om}}^{\text{inv}} + C_{\text{rep}}^{\text{inv}} \quad (11)$$

Once the total cost is calculated, the system cost needs to be determined on an annual basis. In order to determine the annual cost (C_{ann}), C_{tot} must be multiplied by a constant, the capital recovery factor (CRF) as follows [37]:

$$\text{CRF} = \frac{d(1+d)^T}{(1+d)^T - 1} \quad (12)$$

$$C_{\text{ann}} = C_{\text{tot}} \cdot \text{CRF} \quad (13)$$

Once the cost is annualized, the ratio of C_{ann} to the yearly energy provided in kW h (E_{ann}) is calculated as the LCE, given by

$$\text{LCE} = \frac{C_{\text{ann}}}{E_{\text{ann}}} \quad (14)$$

E_{ann} is simply computed by summing all of the energy produced during the yearly simulation as follows:

$$E_{\text{ann}} = \sum_{i=1}^{T_0} p_{\text{load}}(t)dt \quad (15)$$

where T_0 is the number of time steps in the simulation and $p_{\text{load}}(t)$ is the load during a given time step.

2.3.2 Power Demand Constraints. System reliability is often considered in the design of a HPGS. With greater reliability comes the increased cost associated with more storage and generation capability. An often used metric of reliability is loss of power supply probability (LPSP) [2]. LPSP is a measure of the percentage of time a system is not able to supply the required load. In order to satisfy zero LPSP (load is always satisfied), every time step needs to be checked to ensure that the energy available is sufficient to satisfy the load during that period. This is done using the following inequality:

$$c_{\text{bat}}(t) - \text{DoD} \cdot c_{\text{nbat}} + p_{\text{PV}}(t) + p_w(t) - p_{\text{load}}(t) \geq 0 \quad (16)$$

where $c_{\text{bat}}(t-1)$ is the energy storage in the battery at the start of the time step t.

As a summary of this subsection, the complete AIO formulation is presented as follows:

$$\text{HPGS:min LCE}(a_{\text{PV}}, p_r, c_{\text{nbat}})$$

$$\text{with respect to } a_{\text{PV}}, p_r, c_{\text{nbat}}, c_{\text{bat}}(t), \quad \forall\, t = 1, \ldots, T$$

$$\text{such that } c_{\text{bat}}(t) = \text{BU}(c_{\text{bat}}(t-1), p_{\text{PV}}(t), p_w(t), p_{\text{load}}(t)), \quad \forall\, t$$

$$c_{\text{bat}}(t) - \text{DoD} \cdot c_{\text{nbat}} + p_{\text{PV}}(t) + p_w(t) - p_{\text{load}}(t) \geq 0, \quad \forall\, t$$

$$a_{\text{PV}} \geq 0, \quad p_r \geq 0, \quad c_{\text{nbat}} \geq 0 \quad (17)$$

where BU represents the battery update operation. Note that the problem is presented as the sizing optimization of HPGS subject to demand constraints, where the respective capacities of the three major components are taken as design variables and the LCE is minimized. The LCE of the HPGS is calculated through Eqs. (8)–(15), and the reliability of the power supply is evaluated through Eqs. (3)–(7) and (16).

3 Methodology

In this section, a MDO-CC approach for the HPGS design is presented. We first introduce a complementarity reformulation technique, which converts the nonsmooth battery update operation into a set of CCs, and then present a multidisciplinary decomposition approach that solves the derived optimization problem with CCs in a decomposed manner.

3.1 Complementarity Reformulation of Nonsmooth Functions. We note that the battery update operation (Eqs. (6) and (7)), with the if statement, is logically disjunctive in its nature and thus could not be directly represented as a smooth model. Here, we introduce the complementarity reformulation technique for nonsmooth functions, which converts a piecewise smooth function into a set of smooth constraints and CCs with smooth component functions. As a result of this reformulation, optimization problems with these nonsmooth functions could be solved as MPCCs. Motivated by recent developments in MPCC solution algorithms, such reformulation techniques have gained considerable attention over the past decade [23,38,39].

Consider a continuous piecewise smooth function $F(\mathbf{x})$ that is a generalization of the min and max operators as well as the if statement in the battery update operation:

$$F(\mathbf{x}) = F_i(\mathbf{x}) \quad \text{if } a_{i-1} \leq \varphi(\mathbf{x}) \leq a_i, \quad \forall\, i = 1, \ldots, m \quad (18)$$

where $\varphi(\mathbf{x})$ is a switching function, $F_i(\mathbf{x})$ is a smooth function over $\varphi(\mathbf{x})$'s range, and $a_0 \leq a_1 \leq \cdots \leq a_m$ are the switching thresholds. The function has an implicit aspect of discrete selection as it switches between adjacent intervals. In order to facilitate the formulation, we represent the piecewise function as a smooth optimization problem below. Note that the "if" statement in Eq. (18) is converted to a smooth minimization problem, and F obtained through Eq. (19) has the same value with that obtained through Eq. (18) for any $\mathbf{x}$,

$$F(\mathbf{x}) = \sum_{i=1}^{m} F_i(\mathbf{x}) y_i$$

$$\min_{y_i} \sum_{i=1}^{m} (\varphi(\mathbf{x}) - a_{i-1})(\varphi(\mathbf{x}) - a_i) y_i$$

$$\text{such that } \sum_{i=1}^{m} y_i = 1$$

$$y_i \geq 0 \quad (19)$$

We note that there is no integer requirement on y_is, while they take only discrete values in the optimal solution of Eq. (19). The discrete selection is implicitly taken care of by the optimization problem. By replacing the optimization problem (Eq. (19)) with its optimality conditions, which are in the format of CCs, we derive the complementarity reformulation of the piecewise smooth function:

$$F(\mathbf{x}) = \sum_{i=1}^{m} F_i(\mathbf{x}) y_i$$

$$(\varphi(\mathbf{x}) - a_{i-1})(\varphi(\mathbf{x}) - a_i) - \gamma - s_i = 0$$

$$0 \leq y_i \perp s_i \geq 0$$

$$\sum_{i=1}^{m} y_i = 1 \quad (20)$$

where γ and s_i represent the Lagrange multipliers corresponding to the summation and non-negativity constraints, respectively. We note that y_is may take fractional values when φ is equal to one of the thresholds. This problem is trivial for the case of continuous piecewise functions, which are frequently observed in HPGSs.

We note that the battery operation in Eqs. (6) and (7) is an instance of the continuous piecewise smooth function. Therefore, it can be reformulated with the above technique. The reformulated HPGS design problem is presented as follows:

$$\text{HPGS}_{\text{AIO-CC}}:$$

$$\min f = \text{LCE}(a_{\text{PV}}, p_w, c_{\text{nbat}})$$

$$\text{with respect to } a_{\text{PV}}, p_w, c_{\text{nbat}}, c_{\text{bat}}(t), c^*_{\text{bat}}(t), s^-_{\text{net}}(t), s^+_{\text{net}}(t)$$

$$s^-_{\text{b min}}(t), s^+_{\text{b min}}(t), s^-_{\text{b max}}(t), s^+_{\text{b max}}(t), \quad \forall\, t = 1, \ldots, T$$

$$\text{such that } c^*_{\text{bat}}(t) - c_{\text{bat}}(t-1) - \left(- s^-_{\text{net}}(t) \frac{1}{\eta_{\text{dis}}} + s^+_{\text{net}}(t)\, \eta_{\text{ch}} \right) \Delta t = 0, \quad \forall\, t$$

$$p_{\text{PV}}(t)\, \eta_{\text{PV}} + p_w(t)\, \eta_w - \frac{p_{\text{load}}(t)}{\eta_l} - s^+_{\text{net}}(t) + s^-_{\text{net}}(t) = 0, \quad \forall\, t$$

$$0 \le s^-_{\text{net}}(t) \perp s^+_{\text{net}}(t) \ge 0, \quad \forall\, t$$

$$c_{\text{bat}}(t) - c^*_{\text{bat}}(t) - s^-_{\text{bat min}}(t) + s^-_{\text{bat max}}(t) = 0, \quad \forall\, t$$

$$c^*_{\text{bat}}(t) - \text{DoD} \cdot c_{\text{nbat}} - s^+_{\text{bat min}}(t) + s^-_{\text{bat min}}(t) = 0, \quad \forall\, t$$

$$c_{\text{nbat}} - c^*_{\text{bat}}(t) - s^+_{\text{bat max}}(t) + s^-_{\text{bat max}}(t) = 0, \quad \forall\, t$$

$$0 \le s^-_{\text{bat min}}(t) \perp s^+_{\text{bat min}}(t) \ge 0, \quad \forall\, t$$

$$0 \le s^-_{\text{bat max}}(t) \perp s^+_{\text{bat max}}(t) \ge 0, \quad \forall\, t$$

$$a_{\text{PV}} \ge 0, \quad p_w \ge 0, \quad c_{\text{nbat}} \ge 0 \tag{21}$$

where the variables with superscripts + and − are artificial variables introduced to facilitate formulation. They represent the Lagrange multipliers of the intermediate optimization problem in the reformulation. We note that Eq. (21) is an AIO formulation in that all the variables are handled in a single problem.

3.2 Multidisciplinary Decomposition of HPGS Design Optimization Problem. The implementation of the AIO problem is straightforward, but the time dependent variables for battery storage tracking increase the total size of the problem. As the accuracy of the simulation increases, the solution of the AIO problem may become impractical, undesirable, or even impossible. An alternative to the AIO approach is a decomposition-based approach [8], where the original AIO problem is decomposed into a set of inter-related subproblems and solved through an iterative process of subproblem optimization and coordination among them. Using the decomposition-based approach can be advantageous as it breaks the AIO problem into smaller subproblems usually easier to solve while limiting the communication among subproblems only to where necessary via linking variables.

In this subsection, a time horizon decomposition is applied to the AIO HPGS design problem (Eq. (21)), in which the time horizon $\{1, \ldots, T\}$ is split into n consecutive stages, $\{T_{i-1}+1, \ldots, T_i\}_i$, $i=1, \ldots, n$, where $T_0=0$ and $T_n=T$. The derived stages are loosely coupled through the capacity variables and the boundary conditions on the battery storages. Mathematically, this problem falls into the category of a quasi-separable MDO-CC and

Fig. 2 The multidisciplinary optimization model derived from time horizon decomposition

can be solved in a decomposed manner. Specifically, the decomposed structure is composed of n individual stage subproblems (referred to as subsystems), with the ith subsystem dealing with the optimization of the HPGS over the ith time period. The capacity variables, a_{PV}, p_r, and c_{nbat}, are taken as linking variables shared by all the subsystems. In addition, we take the battery storage at the end of each stage $c_{\text{bat}}(T_i)$ as linking variables between subsystems i and $i+1$ to ensure the consistency of the battery storage at the transitions of time periods. An illustration of the multidisciplinary decomposition is shown in Fig. 2.

In order to decompose the AIO problem (Eq. (21)), we introduce a local copy of the linking variables, $a^{(i)}_{\text{PV}}$, $p^{(i)}_r$, $c^{(i)}_{\text{nbat}}$, $c^{(i)}_{\text{bat}}(T_i)$, and $c^{(i)}_{\text{bat}}(T_{i-1})$ to each relevant stage i. In addition, the inconsistency of a linking variable, i.e., the difference between a linking variable and one of its local copies, is penalized by the augmented Lagrangian penalty function: $\phi(y, y^{(i)}) = v^{(i)}(y - y^{(i)}) + (w^{(i)}(y - y^{(i)}))^2$, where y represents one of the above linking variables, $w^{(i)}$ is a weight factor associated with the consistency constraint $h^{(i)} = y - y^{(i)} = 0$, and $v^{(i)}$ is an estimate of the Lagrange multiplier corresponding to $h^{(i)}$. The subscripts PV, w, bat, $i, i+1$, and $i+1, i$ are introduced to differentiate the penalty functions associated with different linking variables. After the relaxation, the derived, loosely coupled problem is further decomposed into a bilevel decomposed formulation, illustrated in Fig. 3. The ith stage of the multistage decomposed formulation is given as

$$\text{HPGS}_{\text{sub},i}:$$

$$\min f^{(i)} + \varepsilon^{(i)} = \text{LCE}(a^{(i)}_{\text{PV}}, p^{(i)}_w, c^{(i)}_{\text{nbat}}) + \varepsilon^{(i)}$$

$$\text{with respect to } \varepsilon^{(i)}, a^{(i)}_{\text{PV}}, p^{(i)}_w, c^{(i)}_{\text{nbat}}, c^{(i)}_{\text{bat}}(T_{i-1}), c^{(i)}_{\text{bat}}(T_i), c_{\text{bat}}(t_i), \quad \forall\, t_i = T_{i-1}+1, \ldots, T_i - 1$$

$$c^*_{\text{bat}}(t_i), s^-_{\text{net}}(t_i), s^+_{\text{net}}(t_i), s^-_{\text{b min}}(t_i), s^+_{\text{b min}}(t_i), s^-_{\text{b max}}(t_i)$$

$$s^+_{\text{b max}}(t_i), \quad \forall\, t_i = T_{i-1}+1, \ldots, T_i$$

$$\text{such that } \phi^{(i)} = \phi^{(i)}_{\text{PV}}(a_{\text{PV}}, a^{(i)}_{\text{PV}}) + \phi^{(i)}_w(p_w, p^{(i)}_w) + \phi^{(i)}_{\text{bat}}(c_{\text{nbat}}, c^{(i)}_{\text{nbat}}) + \phi^{(i)}_{i-1,i}(c_{\text{bat}}(T_{i-1}), c^{(i)}_{\text{bat}}(T_{i-1})) + \phi^{(i)}_{i,i+1}(c_{\text{bat}}(T_i), c^{(i)}_{\text{bat}}(T_i)) \le \varepsilon^{(i)}$$

$$a^{(i)}_{\text{PV}} \ge 0, \quad p^{(i)}_w \ge 0, \quad c^{(i)}_{\text{nbat}} \ge 0$$

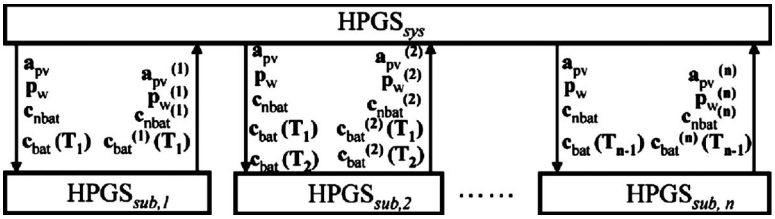

Fig. 3 The decomposition of multistage optimization problem with complementarity constraints

$$c^*_{\text{bat}}(T_{i-1}+1)-c^{(i)}_{\text{bat}}(T_{i-1})+\left(s^-_{\text{net}}(T_{i-1}+1)\frac{1}{\eta_{\text{dis}}}-s^+_{\text{net}}(T_{i-1}+1)\eta_{\text{ch}}\right)\Delta t=0$$

$$c^*_{\text{bat}}(t_i)-c_{\text{bat}}(t_i-1)+\left(s^-_{\text{net}}(t_i)\frac{1}{\eta_{\text{dis}}}-s^+_{\text{net}}(t_i)\eta_{\text{ch}}\right)\Delta t=0,\quad \forall\, t_i=T_{i-1}+2,\ldots,T_i$$

$$p_{\text{PV}}(t_i)\eta_{\text{PV}}+p_w(t_i)\eta_w-\frac{p_{\text{load}}(t_i)}{\eta_l}-s^+_{\text{net}}(t)+s^-_{\text{net}}(t_i)=0,\quad \forall\, t_i$$

$$c_{\text{bat}}(t_i)-c^*_{\text{bat}}(t_i)-s^-_{\text{b min}}(t_i)+s^-_{\text{b max}}(t_i)=0,\quad \forall\, t_i=T_{i-1}+1,\ldots,T_i-1$$

$$c_{\text{bat}}(T_i)-c^*_{\text{bat}}(T_i)-s^-_{\text{b min}}(T_i)+s^-_{\text{b max}}(T_i)=0$$

$$c^*_{\text{bat}}(t_i)-\text{DoD}\cdot c_{\text{nbat}}-s^+_{\text{b min}}(t_i)+s^-_{\text{b min}}(t_i)=0,\quad \forall\, t_i$$

$$c_{\text{nbat}}-c^*_{\text{bat}}(t_i)-s^+_{\text{b max}}(t_i)+s^-_{\text{b max}}(t_i)=0,\quad \forall\, t_i$$

$$0\le s^-_{\text{net}}(t_i)\perp s^+_{\text{net}}(t_i)\ge 0,\quad \forall\, t_i$$

$$0\le s^-_{\text{b min}}(t_i)\perp s^+_{\text{b min}}(t_i)\ge 0,\quad \forall\, t_i$$

$$0\le s^-_{\text{b max}}(t_i)\perp s^+_{\text{b max}}(t_i)\ge 0,\quad \forall\, t_i \tag{22}$$

where $\varepsilon^{(i)}$ is an inconsistency variable to maintain the regularity condition of the deviation constraints [40]. Note that $\phi^{(i)}_{i-1,i}$ in $g^{(i)}_1$ is not included in $g^{(1)}_1$, while $\phi^{(i)}_{i,i+1}$ is not included in $g^{(n)}_1$.

The formulation of the upper level coordination problem is given as

$$\text{HPGS}_{\text{sys}}:$$

$$\min\ \varepsilon$$

$$\text{with respect to } a_{\text{PV}}, p_w, c_{\text{nbat}}$$

$$\text{such that } \phi=\sum_{i=1}^{n}\left(\phi^{(i)}_{\text{PV}}(a_{\text{PV}},a^{(i)}_{\text{PV}})+\phi^{(i)}_w(p_w,p^{(i)}_w)+\phi^{(i)}_{\text{bat}}(c_{\text{nbat}},c^{(i)}_{\text{nbat}})\right)+\sum_{i=2}^{n}\phi^{(i)}_{i-1,i}(c_{\text{bat}}(T_{i-1}),c^{(i)}_{\text{bat}}(T_{i-1}))+\sum_{i=1}^{n-1}\phi^{(i)}_{i,i+1}(c_{\text{bat}}(T_i),c^{(i)}_{\text{bat}}(T_i))\le\varepsilon \tag{23}$$

3.3 Correspondence Between Stationarity Conditions. This subsection is devoted to establishing the correspondence between the stationarity conditions of $\text{HPGS}_{\text{AIO-CC}}$ (Eq. (21)) and the combined stationarity conditions of $\text{HPGS}_{\text{sub},i}$ (Eq. (22)) and HPGS_{sys} (Eq. (23)). Before proceeding, we provide a definition of *strong stationarity*:

DEFINITION 1. *For a generalized MPCC problem,*

$$\text{P}_{\text{MPCC}}:\min_{\mathbf{x}} f(\mathbf{x})$$

$$\mathbf{g}(\mathbf{x})\le\mathbf{0}$$

$$\text{such that } \mathbf{h}(\mathbf{x})=\mathbf{0}$$

$$\mathbf{F}(\mathbf{x})-\mathbf{s}=\mathbf{0}$$

$$\mathbf{G}(\mathbf{x})-\mathbf{t}=\mathbf{0}$$

$$\mathbf{0}\le\mathbf{s}\perp\mathbf{t}\ge\mathbf{0} \tag{24}$$

a point $\mathbf{z}\equiv(\mathbf{x},\mathbf{s},\mathbf{t})$ is strongly stationary if and only if there exist multipliers $(\boldsymbol{\mu},\boldsymbol{\lambda},\boldsymbol{\sigma}_1,\boldsymbol{\sigma}_2,\boldsymbol{\nu}_1,\boldsymbol{\nu}_2)$, satisfying

$$\begin{pmatrix}\nabla f\\ \mathbf{0}\\ \mathbf{0}\end{pmatrix}+\begin{pmatrix}\nabla g & \mathbf{0} & \mathbf{0}\\ \nabla h & \mathbf{0} & \mathbf{0}\\ \nabla F & -I & \mathbf{0}\\ \nabla G & -I & \mathbf{0}\end{pmatrix}^T\begin{pmatrix}\boldsymbol{\mu}\\ \boldsymbol{\lambda}\\ \boldsymbol{\sigma}_1\\ \boldsymbol{\sigma}_2\end{pmatrix}-\begin{pmatrix}\mathbf{0}\\ \boldsymbol{\nu}_1\\ \boldsymbol{\nu}_2\end{pmatrix}=\mathbf{0}$$

$$\mathbf{0}\le\boldsymbol{\mu}\perp-\mathbf{g}(\mathbf{x})\ge\mathbf{0}$$

$$\mathbf{h}(\mathbf{x})=\mathbf{0}$$

$$\mathbf{F}(\mathbf{x})-\mathbf{s}=\mathbf{0}$$

$$\mathbf{G}(\mathbf{x})-\mathbf{t}=\mathbf{0}$$

$$\mathbf{0}\le\mathbf{s}\perp\mathbf{t}\ge\mathbf{0}$$

$$[\boldsymbol{\nu}_1]_j[\mathbf{s}]_j=0,\quad\forall\, j$$

$$[\boldsymbol{\nu}_2]_j[\mathbf{t}]_j=0,\quad\forall\, j$$

$$\text{if } [\mathbf{s}]_j=[\mathbf{t}]_j=0\quad\text{then } [\nu_1]_j\ge 0\ \text{ and }\ [\nu_2]_j\ge 0,\quad\forall\, j \tag{25}$$

Suppose $\mathcal{A}_1,\mathcal{A}_2\subseteq\{1,\ldots,n\}$ are the sets of indices corresponding to s and t, respectively. Then, these sets can be employed to construct a relaxed nonlinear program:

$$\text{P}_{\text{MPCC-RNLP}}:\min_{\mathbf{x}} f(\mathbf{x})$$

$$\text{such that } \mathbf{g}(\mathbf{x})\le\mathbf{0}$$

$$\mathbf{h}(\mathbf{x})=\mathbf{0}$$

$$\mathbf{G}(\mathbf{x})-\mathbf{s}=\mathbf{0}$$

$$\mathbf{F}(\mathbf{x})-\mathbf{t}=\mathbf{0}$$

$$[\mathbf{s}]_j=\mathbf{0},\quad\forall\, j\in\mathcal{A}_2^{\perp}$$

$$[\mathbf{t}]_j=\mathbf{0},\quad\forall\, j\in\mathcal{A}_1^{\perp}$$

$$[\mathbf{s}]_j\ge\mathbf{0},\quad\forall\, j\in\mathcal{A}_1$$

$$[\mathbf{t}]_j\ge\mathbf{0},\quad\forall\, j\in\mathcal{A}_2 \tag{26}$$

The notion of strong-stationarity is intimately related to the relaxed NLP in that a point is a strong-stationary solution of P_{MPCC} if and only if it is a stationary point of $\text{P}_{\text{MPCC-RNLP}}$ (see Prop. 4.1 [19]). Furthermore, a point satisfies second-order strong-stationarity conditions of P_{MPCC} if and only if it satisfies second-order sufficient conditions (SOSCs) for the relaxed NLP $\text{P}_{\text{MPCC-RNLP}}$.

We note that the complementarity formulation of the HPGS design optimization problem falls into the category of MDO-CC, whose formulation is given as follows:

$$\text{P}_{\text{MDO-CC-AIO}}:$$

$$\min_{\mathbf{y},\mathbf{x}_1,\ldots,\mathbf{x}_n}\sum_{i=1}^{n} f_i(\mathbf{x}_i,\mathbf{y})$$

$$\text{such that } \mathbf{g}_i(\mathbf{x}_i,\mathbf{y})\le\mathbf{0},\quad\forall\, i=1,\ldots,n$$

$$\mathbf{h}_i(\mathbf{x}_i,\mathbf{y})=\mathbf{0},\quad\forall\, i=1,\ldots,n$$

$$\mathbf{0} \le \mathbf{G}_i(\mathbf{x}_i,\mathbf{y}) \perp \mathbf{F}_i(\mathbf{x}_i,\mathbf{y}) \ge \mathbf{0}, \quad \forall\, i = 1, \ldots, n \tag{27}$$

where $\mathbf{y}$ represents a vector of linking variables shared by all the n subsystems, and $\mathbf{x}_i$ represents the vector of local variables only relevant to subsystem i, $i=1,\ldots,n$. Additionally, $f_i(\mathbf{x}_i,\mathbf{y})$ represents the local objective of subsystem i, which depends on the linking variables $\mathbf{y}$ and the local variables $\mathbf{x}_i$. Similarly, local constraint functions are given as $\mathbf{g}_i(\mathbf{x}_i,\mathbf{y})$, $\mathbf{h}_i(\mathbf{x}_i,\mathbf{y})$, $\mathbf{F}_i(\mathbf{x}_i,\mathbf{y})$, and $\mathbf{G}_i(\mathbf{x}_i,\mathbf{y})$. The objective and constraint functions are assumed to be twice continuously differentiable functions.

By applying the decomposition technique in the previous subsection, the AIO MDO-CC problem (Eq. (27)) can be decomposed into a bilevel formulation similar to the one presented in Fig. 3. Specifically, the formulation of the ith subsystem and that of the system level problem are shown as follows:

$$\mathrm{P}_{\text{MDO-CC-Subsys},i}\text{: } \min_{\mathbf{y}_i,\mathbf{x}_i,\varepsilon_i} f_i(\mathbf{x}_i,\mathbf{y}_i) + \varepsilon_i$$

$$\text{such that } \phi_i(\mathbf{y},\mathbf{y}_i) \le \varepsilon_i$$

$$\mathbf{g}_i(\mathbf{x}_i,\mathbf{y}_i) \le \mathbf{0}$$

$$\mathbf{h}_i(\mathbf{x}_i,\mathbf{y}_i) = \mathbf{0}$$

$$\mathbf{0} \le \mathbf{G}_i(\mathbf{x}_i,\mathbf{y}_i) \perp \mathbf{F}_i(\mathbf{x}_i,\mathbf{y}_i) \ge \mathbf{0} \tag{28}$$

$$\mathrm{P}_{\text{MDO-CC-Sys}}\text{:} \min_{\mathbf{y},\varepsilon} \varepsilon$$

$$\text{such that } \sum_{i=1}^{n} \phi_i(\mathbf{y},\mathbf{y}_i) \le \varepsilon \tag{29}$$

where y_i is a local copy of the linking variables in subsystem i.

We note that complementarity formulation of the HPGS design optimization problem (Eq. (21)) is a special case of the MDO-CC problem (Eq. (27)); correspondingly, its decomposed formulation (Eqs. (22) and (23)) is a special case of that given in Eqs. (28) and (29) (to see this, let $\mathbf{y}=[a_{\mathrm{PV}},p_w,c_{\mathrm{nbat}},c_{\mathrm{bat}}(T_1),\ldots,c_{\mathrm{bat}}(T_{n-1})]^T$ and $\mathbf{x}_i=[c_{\mathrm{bat}}(T_{i-1}+1),\ldots,c_{\mathrm{bat}}(T_i-1),c^*_{\mathrm{bat}}(T_{i-1}+1),\ldots,c^*_{\mathrm{bat}}(T_i)]^T$). Therefore, the correspondence between the stationarity conditions of Eq. (21) and those of Eqs. (22) and (23) follows the correspondence between the stationarity conditions of Eq. (27) and those of Eqs. (28) and (29). The following theorem establishes this correspondence between the first-order stationarity conditions.

THEOREM 1. *Let* $(\mathbf{x}_1,\ldots,\mathbf{x}_n,\mathbf{y}_1,\ldots,\mathbf{y}_n,\varepsilon_1,\ldots,\varepsilon_n,\mathbf{y},\varepsilon)$ be an accumulation of strongly stationary points of $\mathrm{P}_{\text{MDO-CC-Subsys},i}$ and a stationary point of $\mathrm{P}_{\text{MDO-CC-Sys}}$. If it satisfies $\mathbf{y}=\mathbf{y}_1=\cdots=\mathbf{y}_m$, then $(\mathbf{x}_1,\ldots,\mathbf{x}_m,\mathbf{y})$ is a strongly stationary point of $\mathrm{P}_{\text{MDO-CC-AIO}}$.

Proof. Note that problem $\mathrm{P}_{\text{MDO-CC-Subsys},i}$ can be restated as follows:

$$\mathrm{P}'_{\text{MDO-CC-Subsys},i}\text{: } \min_{\mathbf{y}_i,\mathbf{x}_i,\mathbf{s}_i,\mathbf{t}_i,\varepsilon_i} f_i(\mathbf{x}_i,\mathbf{y}_i) + \varepsilon_i$$

$$\text{such that } \phi_i(\mathbf{y},\mathbf{y}_i) \le \varepsilon_i, \quad (\zeta_i) \tag{30}$$

$$\mathbf{g}_i(\mathbf{x}_i,\mathbf{y}_i) \le \mathbf{0}, \quad (\mu_i) \tag{31}$$

$$\mathbf{h}_i(\mathbf{x}_i,\mathbf{y}_i) = \mathbf{0}, \quad (\lambda_i) \tag{32}$$

$$\mathbf{G}_i(\mathbf{x}_i,\mathbf{y}_i) - \mathbf{s}_i = \mathbf{0}, \quad (\sigma_{i1}) \tag{33}$$

$$\mathbf{F}_i(\mathbf{x}_i,\mathbf{y}_i) - \mathbf{t}_i = \mathbf{0}, \quad (\sigma_{i2}) \tag{34}$$

$$\mathbf{0} \le \mathbf{s}_i \perp \mathbf{t}_i \ge \mathbf{0} \tag{35}$$

Following Definition 1, the strong stationarity conditions of $\mathrm{P}'_{\text{MDO-CC-Subsys},i}$ in Eq. (30) is given as

$$\begin{pmatrix} \nabla_{\mathbf{y}_i} f_i \\ \nabla_{\mathbf{x}_i} f_i \\ \mathbf{0} \\ \mathbf{0} \\ 1 \end{pmatrix} + \begin{pmatrix} \nabla_{\mathbf{y}_i}\mathbf{g}_i & \nabla_{\mathbf{x}_i}\mathbf{g}_i & \mathbf{0} & \mathbf{0} & 0 \\ \nabla_{\mathbf{y}_i}\phi_i^T & \mathbf{0} & \mathbf{0} & \mathbf{0} & -1 \end{pmatrix}^T \begin{pmatrix} \boldsymbol{\mu}_i \\ \zeta_i \end{pmatrix}$$

$$+ \begin{pmatrix} \nabla_{\mathbf{y}_i}\mathbf{h}_i & \nabla_{\mathbf{x}_i}\mathbf{h}_i & \mathbf{0} & \mathbf{0} & 0 \\ \nabla_{\mathbf{y}_i}\mathbf{G}_i & \nabla_{\mathbf{x}_i}\mathbf{G}_i & -\mathbf{I} & \mathbf{0} & 0 \\ \nabla_{\mathbf{y}_i}\mathbf{F}_i & \nabla_{\mathbf{x}_i}\mathbf{F}_i & \mathbf{0} & -\mathbf{I} & 0 \end{pmatrix}^T \begin{pmatrix} \lambda_i \\ \boldsymbol{\sigma}_{i1} \\ \boldsymbol{\sigma}_{i2} \end{pmatrix} - \begin{pmatrix} \mathbf{0} \\ \mathbf{0} \\ \boldsymbol{\nu}_{i1} \\ \boldsymbol{\nu}_{i2} \\ 0 \end{pmatrix} = \mathbf{0}$$

$$0 \le \zeta_i \perp \varepsilon_i - \phi_i(\mathbf{y},\mathbf{y}_i) \ge 0$$

$$\mathbf{0} \le \boldsymbol{\mu}_i \perp -\mathbf{g}_i(\mathbf{x}_i,\mathbf{y}_i) \ge \mathbf{0}$$

$$\mathbf{h}_i(\mathbf{x}_i,\mathbf{y}_i) = \mathbf{0}$$

$$\mathbf{G}_i(\mathbf{x}_i,\mathbf{y}_i) - \mathbf{s}_i = \mathbf{0}$$

$$\mathbf{F}_i(\mathbf{x}_i,\mathbf{y}_i) - \mathbf{t}_i = \mathbf{0}$$

$$\mathbf{0} \le \mathbf{s}_i \perp \mathbf{t}_i \ge \mathbf{0}$$

$$[\boldsymbol{\nu}_{i1}]_j[\mathbf{s}_i]_j = 0, \quad \forall\, j$$

$$[\boldsymbol{\nu}_{i2}]_j[\mathbf{t}_i]_j = 0, \quad \forall\, j$$

$$\text{if } [\mathbf{s}_i]_j = [\mathbf{t}_i]_j = 0 \quad \text{then } [\nu_{i1}]_j \ge 0 \text{ and } [\nu_{i2}]_j \ge 0, \quad \forall\, j \tag{36}$$

where the symbol ∇ denotes a gradient for scalar functions and the Jacobian for vector functions. We note that for the last row in Eq. (36) to be satisfied, the scalar Lagrange multiplier corresponding to the consistency penalty constraint, ζ_i, must be equal to 1. Therefore, the consistency penalty constraint is active at strongly stationary points of $\mathrm{P}'_{\text{MDO-CC-Subsys},i}$.

In order to consider the set of strong-stationary conditions of all the subsystems, we sum up the equations corresponding to $\mathbf{y}_i$ from Eq. (36) for each subsystem and derive the following system:

$$\sum_{i=1}^{n} \nabla_{\mathbf{y}_i} f_i + \sum_{i=1}^{n} \nabla_{\mathbf{y}_i}\phi_i + \sum_{i=1}^{n} (\nabla_{\mathbf{y}_i}\mathbf{g}_i)^T\boldsymbol{\mu}_i + \sum_{i=1}^{n} \begin{pmatrix} \nabla_{\mathbf{y}_i}\mathbf{h}_i \\ \nabla_{\mathbf{y}_i}\mathbf{G}_i \\ \nabla_{\mathbf{y}_i}\mathbf{F}_i \end{pmatrix}^T \begin{pmatrix} \boldsymbol{\lambda}_i \\ \boldsymbol{\sigma}_{i1} \\ \boldsymbol{\sigma}_{i2} \end{pmatrix} = \mathbf{0} \tag{37}$$

The stationarity conditions of $\mathrm{P}_{\text{MDO-CC-Sys}}$ in Eq. (29) are given as

$$\begin{pmatrix} \mathbf{0} \\ 1 \end{pmatrix} + \left(\sum_{i=1}^{n} \nabla_{\mathbf{y}}\phi_i^T - 1 \right)^T \tau = \mathbf{0} \tag{38}$$

$$0 \le \tau \perp \varepsilon - \sum_{i=1}^{n} \phi_i(\mathbf{y},\mathbf{y}_i) \ge 0 \tag{39}$$

Again, the scalar Lagrange multiplier τ has to be 1, so that the last row in Eq. (38) is satisfied.

Note that under the consistency assumption $\mathbf{y}=\mathbf{y}_1=\cdots=\mathbf{y}_m$, $\nabla^T_{\mathbf{y}}\phi_i=-\nabla^T_{\mathbf{y}_i}\phi_i$ holds for both the augmented Lagrangian penalty function and the quadratic penalty function. Substituting this result into Eq. (38), we have

$$\sum_{i=1}^{n} \nabla_{\mathbf{y}_i}\phi_i = \mathbf{0} \tag{40}$$

Therefore, the second term in Eq. (37) cancels.

Given $\mathbf{y}=\mathbf{y}_i$, it is straightforward that

$$f_i(\mathbf{x}_i,\mathbf{y}_i)=f_i(\mathbf{x}_i,\mathbf{y}),\quad \nabla_{\mathbf{y}_i}f_i(\mathbf{x}_i,\mathbf{y}_i)=\nabla_{\mathbf{y}}f_i(\mathbf{x}_i,\mathbf{y}) \tag{41}$$

Similar results follow for $\mathbf{g}_i$, $\mathbf{h}_i$, $\mathbf{G}_i$, and $\mathbf{F}_i$.

Summarizing Eqs. (36), (37), and (41), we have

$$\begin{pmatrix} \sum_{i=1}^{n}\nabla_{\mathbf{y}}\mathbf{g}_i & \nabla_{\mathbf{x}_1}\mathbf{g}_1 & \cdots & \nabla_{\mathbf{x}_n}\mathbf{g}_n & \mathbf{0} & \mathbf{0} \\ \sum_{i=1}^{n}\nabla_{\mathbf{y}}\mathbf{h}_i & \nabla_{\mathbf{x}_1}\mathbf{h}_1 & \cdots & \nabla_{\mathbf{x}_n}\mathbf{h}_n & \mathbf{0} & \mathbf{0} \\ \sum_{i=1}^{n}\nabla_{\mathbf{y}}\mathbf{G}_i & \nabla_{\mathbf{x}_1}\mathbf{G}_1 & \cdots & \nabla_{\mathbf{x}_n}\mathbf{G}_n & -\mathbf{I} & \mathbf{0} \\ \sum_{i=1}^{n}\nabla_{\mathbf{y}}\mathbf{F}_i & \nabla_{\mathbf{x}_1}\mathbf{F}_1 & \cdots & \nabla_{\mathbf{x}_n}\mathbf{F}_n & \mathbf{0} & -\mathbf{I} \end{pmatrix}^T \begin{pmatrix} \boldsymbol{\mu}_i \\ \boldsymbol{\lambda} \\ \boldsymbol{\sigma}_1 \\ \boldsymbol{\sigma}_2 \end{pmatrix} + \begin{pmatrix} \sum_{i=1}^{n}\nabla_{\mathbf{y}}f_i \\ \nabla_{\mathbf{x}_1}f_1 \\ \vdots \\ \nabla_{\mathbf{x}_n}f_n \\ \mathbf{0} \\ \mathbf{0} \end{pmatrix} - \begin{pmatrix} \mathbf{0} \\ \mathbf{0} \\ \vdots \\ \mathbf{0} \\ \boldsymbol{\nu}_1 \\ \boldsymbol{\nu}_2 \end{pmatrix} = \mathbf{0}$$

$$\mathbf{0}\le\boldsymbol{\mu}_i\perp -\mathbf{g}_i(\mathbf{x}_i,\mathbf{y})\ge\mathbf{0},\quad \forall\, i$$

$$\mathbf{h}_i(\mathbf{x}_i,\mathbf{y})=\mathbf{0},\quad \forall\, i$$

$$\mathbf{G}_i(\mathbf{x}_i,\mathbf{y})-\mathbf{s}_i=\mathbf{0},\quad \forall\, i$$

$$\mathbf{F}_i(\mathbf{x}_i,\mathbf{y})-\mathbf{t}_i=\mathbf{0},\quad \forall\, i$$

$$\mathbf{0}\le\mathbf{s}_i\perp\mathbf{t}_i\ge\mathbf{0},\quad \forall\, i$$

$$[\boldsymbol{\nu}_{i1}]_j[\mathbf{s}_i]_j=0,\quad \forall\, i,j$$

$$[\boldsymbol{\nu}_{i2}]_j[\mathbf{t}_i]_j=0,\quad \forall\, i,j$$

$$\text{if } [\mathbf{s}_i]_j=[\mathbf{t}_i]_j=0 \text{ then } [\boldsymbol{\nu}_{i1}]_j\ge 0 \text{ and } [\boldsymbol{\nu}_{i2}]_j\ge 0,\quad \forall\, i,j \tag{42}$$

where $\boldsymbol{\lambda}=[\boldsymbol{\lambda}_1^T,\ldots,\boldsymbol{\lambda}_n^T]^T$, $\boldsymbol{\sigma}_1=[\boldsymbol{\sigma}_{11}^T,\ldots,\boldsymbol{\sigma}_{n1}^T]^T$,

$\boldsymbol{\sigma}_2=[\boldsymbol{\sigma}_{12}^T,\ldots,\boldsymbol{\sigma}_{n2}^T]^T$, $\boldsymbol{\nu}_1=[\boldsymbol{\nu}_{11}^T,\ldots,\boldsymbol{\nu}_{n1}^T]^T$, $\boldsymbol{\nu}_2=[\boldsymbol{\nu}_{12}^T,\ldots,\boldsymbol{\nu}_{n2}^T]^T$

Note that Eq. (43) is exactly the strong-stationarity conditions of the following problem:

$$\mathrm{P}'_{\text{MDO-CC-AIO}}:$$

$$\min_{\mathbf{y},\mathbf{x}_1,\ldots,\mathbf{x}_n}\ \sum_{i=1}^{n} f_i(\mathbf{x}_i,\mathbf{y})$$

$$\text{such that } \mathbf{g}_i(\mathbf{x}_i,\mathbf{y})\le\mathbf{0},\quad \forall\, i=1,\ldots,n$$

$$\mathbf{h}_i(\mathbf{x}_i,\mathbf{y})=\mathbf{0},\quad \forall\, i=1,\ldots,n$$

$$\mathbf{G}_i(\mathbf{x}_i,\mathbf{y})-\mathbf{s}_i=\mathbf{0},\quad \forall\, i=1,\ldots,n$$

$$\mathbf{F}_i(\mathbf{x}_i,\mathbf{y})-\mathbf{t}_i=\mathbf{0},\quad \forall\, i=1,\ldots,n$$

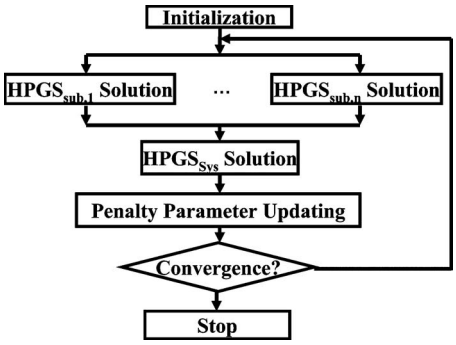

Fig. 4 Alternating direction method of multiplier for HPGS design optimization

$$\mathbf{0}\le\mathbf{s}_i\perp\mathbf{t}_i\ge\mathbf{0},\quad \forall\, i=1,\ldots,n \tag{43}$$

This is just a restatement of $\mathrm{P}_{\text{MDO-CC-AIO}}$ (Eq. (27)), giving us the required equivalence result. □

3.4 Solution Algorithm. We note that the decomposed formulation of the MDO-CC problem in Eqs. (23) and (22) is parametrized by weighting factors. Solving the decomposed problem under fixed weights does not usually lead to feasible solutions of the original AIO problem. Therefore, a weight updating scheme is necessary so that the successive solutions of the decomposed formulation converge to an optimal solution of the original AIO problem.

We follow the alternating direction method of multipliers [16,41], as shown in Fig. 4: In each iteration, the subsystem (lower) level subproblems (Eq. (22)) are first solved either sequentially or parallel under fixed penalty parameters; then, the system (upper) level subproblem in Eq. (23) is solved under the same penalty parameter settings. After that, the penalty parameters are updated based on the violation of the linking variable consistencies. Under the augmented Lagrangian formulation, the violation of a consistency constraint $h_*^{(i)}=y_*-y_*^{(i)}=0$, where y_* represents one of the linking variables, can be reduced by taking the corresponding Lagrange multiplier estimate $v_*^{(i)}$ close to the optimal Lagrange multiplier $\lambda_*^{(i)}$ corresponding to $h_*^{(i)}$. In order to achieve this, a linear updating scheme for selecting vectors $v_*^{(i)}$ is given by

$$(v_*^{(i)})^{(k)}=(v_*^{(i)})^{(k)}+2(w_*^{(i)})^{(k)}(w_*^{(i)})^{(k)}(h_*^{(i)})^{(k)},\quad i=1,\ldots,p \tag{44}$$

where the superscript (k) indicates the value of a variable at the ith iteration. Additionally, the weight vector is updated following a linear growth formula:

$$(w_*^{(i)})^{(k+1)}=\beta\cdot(w_*^{(i)})^{(k)},\quad i=1,\ldots,p \tag{45}$$

Finally, we provide some recommendations for the selection of β. While $2<\beta<3$ is usually recommended for the augmented Lagrangian approach with nested loop implementation [42,43], our numerical experience indicates that a more moderate value is required for the alternating direction implementation. Generally, $1<\beta<1.1$ is recommended for the speed of the convergence.

4 Numerical Study

In this section, a demonstrative HPGS design case study is presented to validate the presented MDO-CC approach.

4.1 Demonstration Case. We consider a stand-alone hybrid PV/wind power generation system located at Ersa on Corsica Island, France, which is adopted from a series of papers produced by Diaf et al. [44,45,30] on HPGS design. The monthly resource

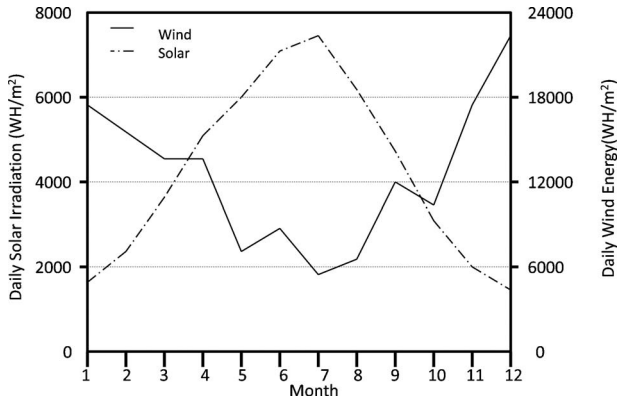

Fig. 5 Energy resources at Ersa on Corsica Island, France

data from Ref. [30] are shown in Fig. 5.

A daily simulation is employed to track the performance of the HPGS. In order to generate daily resource data, tools from the software package HOMER were used [46]. HOMER allows users to input monthly averages of wind and solar resources and outputs corresponding synthetic hourly values. For both resources, the only values altered from the HOMER defaults were the monthly averages. Other parameters describing the distributions were left at the HOMER defaults. The hourly values were then exported from HOMER and summed over 24 h periods to give units of W/m^2 day. These series were then used as the resource inputs to the model.

In addition to the resource inputs, the required energy to satisfy the load is also necessary. Because energy demand is often dependent on external factors (e.g., weather conditions), seasonal averages were used. The demand for summer, winter, and spring/autumn are 3436, 4230, and 3844 W h/day, respectively.

Table 1 Battery, invertor, and PV parameters

η_{ch}	η_{dis}	DoD	η_l	η_{PV}	η_g
0.75	1	80%	0.95	0.95	0.123

Table 2 Wind generator parameters

V_{in}	V_r	V_{out}	η_w
2.5 m/s	12 m/s	25 m/s	0.95

Table 3 Cost parameters [47]

	C_{unit} ($/W)	Install (%)	O&M (%)	L_{comp} (yr)	g	d
Wind	3.00	20	3	20	0.05	0.08
PV	4.84	40	1	25	0.05	0.08
Batteries	0.190	–	–	4	0.05	0.08
Inverter	0.713	–	1	10	0.05	0.08

Another set of necessary inputs are the parameters for the component models. These are listed in Tables 1 and 2. Table 3 shows the pricing parameters used to calculate the cost of the system. These values will be dependent on system location and local component pricing. The parameters g and d were assumed to be the same for all components, while the other values were component dependent. For the Install %, O&M %, and L_{comp} parameters, the same assumptions were used as in Ref. [30]. The C_{unit} values were averages obtained from an industry website [47].

4.2 Numerical Results. In order to analyze its numerical behavior, the presented approach is applied to the demonstrative HPGS design optimization case with varying granularity of decomposition (i.e., number of stages). For each of the two decomposition settings tested (two and four stages), the decomposition method obtains a solution that is identical to the AIO solution numerically generated from the same initial point. According to the obtained solution, the optimal capacities of the three components are $[a_{PV}, p_r, c_{nbat}]=[3.9439, 0.9104, 3.0239]$, where the three metrics are in m^2, kW, and kW h, respectively. This design corresponds to a LCE of \$0.8397/kW h.

For each decomposition setting, the presented algorithm is terminated when the scaled consistency deviation of the linking variables:

$$\frac{\sum_{i=1}^{n} \|\mathbf{y} - \mathbf{y}^{(i)}\|_2}{1 + \|\mathbf{y}\|_2} \tag{46}$$

is less then 1×10^{-6}, where $\mathbf{y}$ indicates the linking variables. Here, the problem is scaled so that each element of the linking variable has a magnitude of 1. The number of function evaluations and the computation time taken to converge for each setting are presented in Table 4. Note that the parallel function evaluations are measured by summing up the maximum number of subsystem function evaluation out of each iteration. Additionally, the scaled deviations between the AIO solutions and the decomposition solutions,

$$\frac{\|\mathbf{x}_{AIO} - \mathbf{x}_{decomp}\|_2}{1 + \|\mathbf{x}_{AIO}\|_2} \tag{47}$$

is also presented. Each optimization setting is implemented with KNITRO®5.0 solver in MATLAB®7.2. with a β value of 1.002.

As shown in Table 4, the computation time of the two-stage decomposition approach is approximately 45% less than the that of the AIO approach, while the computation time of the four-stage decomposition approach is slightly less than that of the AIO approach. This result indicates that there is a trade-off between the reduced subproblem size and the increased complexity of coordination. Note that the computation time of the decomposition algorithm is measured under serial implementation; i.e., the computation time is the summation of all the subsystem computation time. If the algorithm is implemented in parallel, the computation time will be much shorter. This work provides a framework for future application to larger system-of-system problems, such as optimizing the layout and sizing of a hybrid energy network or

Table 4 The numerical behavior of the ALD algorithm

Solution setting	No. of function evaluations (NFE): Serial	NFE: parallel	Computation time (s)	Deviation from AIO solution
AIO	1.135×10^7	–	5.577×10^3	–
Decomposition: two stages	7.128×10^6	4.354×10^6	3.104×10^3	6.37×10^{-4}
Decomposition: four stages	6.053×10^6	2.423×10^6	5.469×10^3	8.62×10^{-4}

energy farm. For such problems, the decomposed MPCC formulation could show significant improvement over current methods, which is addressed in the next section.

5 Conclusion and Future Works

MDO-CC is an extension to traditional MDO models, which is motivated by capturing multidisciplinary system working under (and switching among) multiple working modes as well as by considering game equilibriums, such as market competition and interaction among multiple design teams in the context of MDO. This paper presents a MDO-CC approach for HPGS design optimization. HPGS design optimization involves discrete-time simulation with logically disjunctive operations and time dependent variables, which usually leads to a nonsmooth model with increased problem size. Therefore, traditional optimization techniques may have difficulties applying to this type of problem. The presented approach reformulates the logically disjunctive battery update operations into complementarity constraints and employs a multidisciplinary decomposition algorithm to solve the reformulated problem. In addition, the correspondence between the stationarity conditions of the original AIO problem and those of the decomposed problem is established. A numerical study of the hybrid PV/wind power generation system shows that it converges to solutions identical to the AIO solutions. Our future work in HPGS design optimization will include introducing the wake effect of the wind module in the energy farm setting and supplemental diesel power generation. It would also be an interesting research topic to consider the probabilistic performance analysis of the HPGS in conjunction with a system reliability assessment.

Acknowledgment

This material is based upon work supported by the National Science Foundation under under Award Nos. 0728863 (Shanbhag) and 0900196 (Kim). Any opinions, findings, conclusions, or recommendations are those of the author(s) and do not necessarily reflect the views of the National Science Foundation. The authors also acknowledge constructive feedback by Dr. Christopher Ha, Dr. Jalaja Repalle, and Dr. Todd Benanzer at the Caterpillar Champaign Simulation Center.

References

[1] Nema, P., Nema, R., and Rangnekar, S., 2009, "A Current and Future State of Art Development of Hybrid Energy System Using Wind and PV-Solar: A Review," Renewable Sustainable Energy Rev., **13**(8), pp. 2096–2103.
[2] Zhou, W., Lou, C., Li, Z., Lu, L., and Yang, H., 2010, "Current Status of Research on Optimum Sizing of Stand-Alone Hybrid Solar-Wind Power Generation Systems," Appl. Energy, **87**(2), pp. 380–389.
[3] Borowy, B. S., and Salameh, Z. M., 1996, "Methodology for Optimally Sizing the Combination of a Battery Bank and PV Array in a Wind/PV Hybrid System," IEEE Trans. Energy Convers., **11**(2), pp. 367–375.
[4] Reddy, J., and Reddy, D., 2004, "Probabilistic Performance Assessment of a Roof Top Wind, Solar Photo Voltaic Hybrid Energy System," Reliability and Maintainability, 2004 Annual Symposium—RAMS, pp. 654–658.
[5] Valenciaga, F., Puleston, P., Battaiotto, P., and Mantz, R., 2000, "Passivity/Sliding Mode Control of a Stand-Alone Hybrid Generation System," IEE Proc.: Control Theory Appl., **147**(6), pp. 680–686.
[6] Koutroulis, E., Kolokotsa, D., Potirakis, A., and Kalaitzakis, K., 2006, "Methodology for Optimal Sizing of Stand-Alone Photovoltaic/Wind-Generator Systems Using Genetic Algorithms," Sol. Energy, **80**(9), pp. 1072–1088.
[7] Lu, S., and Kim, H. M., 2010, "A Regularized Inexact Penalty Decomposition Algorithm for Multidisciplinary Design Optimization Problem With Complementarity Constraints," ASME J. Mech. Des., **132**(4), p. 041005.
[8] Balling, R. J., and Sobieszczanski-Sobieski, J., 1996, "Optimization of Coupled Systems: A Critical Overview of Approaches," AIAA J., **34**(1), pp. 6–17.
[9] Hussaini, M. Y., and Alexandrov, N. M., eds., 1997, *Multidisciplinary Design Optimization: State of the Art* (*Proceedings of the ICASE/NASA Langley Workshop on Multidisciplinary Design Optimization*, Hampton, VA, March 13-16, SIAM, Philadelphia, PA.
[10] Sobieszczanski-Sobieski, J., 1988, "Optimization by Decomposition: A Step From Hierarchic to Non-Hierarchic Systems," The Second NASA Air Force Symposium on Recent Advances in Multidisciplinary Analysis and Optimization, Paper No. NASA-CP 3031.
[11] Sobieszczanski-Sobieski, J., Agte, J., and Sandusky, R., Jr., 2000, "Bilevel Integrated System Synthesis," AIAA J., **38**(1), pp. 164–172.
[12] Braun, R., 1996, "Collaborative Optimization: An Architecture for Large-Scale Distributed Design," Ph.D. thesis, Stanford University, Stanford, CA.
[13] Haftka, R., and Watson, L., 2005, "Multidisciplinary Design Optimization With Quasiseparable Subsystems," Optim. Eng., **6**, pp. 9–20.
[14] Kim, H. M., 2001, "Target Cascading in Optimal System Design," Ph.D. thesis, Mechanical Engineering Department, University of Michigan, Ann Arbor, MI.
[15] DeMiguel, V., and Murray, W., 2006, "A Local Convergence Analysis of Bilevel Programming Decomposition Algorithms," Optim. Eng., **7**(2), pp. 99–133.
[16] Tosserams, S., Etman, L. F. P., and Rooda, J. E., 2007, "An Augmented Lagrangian Decomposition Method for Quasiseparable Problems in MDO," Struct. Multidiscip. Optim., **34**(3), pp. 211–227.
[17] Lu, S., Kim, H. M., Norato, J., and Ha, C., 2008, "Analytical Target Cascading for Multi-Mode Design Optimization: An Engine Case Study," Proceedings of the Fourth AIAA Multidisciplinary Design Optimization Specialist Conference.
[18] Nocedal, J., and Wright, S. J., 1999, *Numerical Optimization*, Springer Series in Operations Research, Springer-Verlag, New York.
[19] Fletcher, R., Leyffer, S., Ralph, D., and Scholtes, S., 2006, "Local Convergence of SQP Methods for Mathematical Programs With Equilibrium Constraints," SIAM J. Optim., **17**(1), pp. 259–286.
[20] Anitescu, M., 2005, "On Solving Mathematical Programs With Complementarity Constraints as Nonlinear Programs," SIAM J. Optim., **15**(4), pp. 1203–1236.
[21] Hu, X. M., and Ralph, D., 2004, "Convergence of a Penalty Method For Mathematical Programming With Complementarity Constraints," J. Optim. Theory Appl., **123**(2), pp. 365–390.
[22] Leyffer, S., Lopez-Calva, G., and Nocedal, J., 2006, "Interior Methods for Mathematical Programs With Complementarity Constraints," SIAM J. Optim., **17**(1), pp. 52–77.
[23] Luo, Z.-Q., Pang, J.-S., and Ralph, D., 1996, *Mathematical Programs With Equilibrium Constraints*, Cambridge University Press, Cambridge, UK.
[24] Liu, X., and Sun, J., 2004, "A New Decomposition Technique in Solving Multistage Stochastic Linear Programs by Infeasible Interior Point Methods," J. Global Optim., **28**(2), pp. 197–215.
[25] Raghunathan, A. U., and Biegler, L. T., 2005, "An Interior Point Method for Mathematical Programs With Complementarity Constraints (MPCCs)," SIAM J. Optim., **15**(3), pp. 720–750.
[26] Shanbhag, U. V., 2006, "Decomposition and Sampling Methods for Stochastic Equilibrium Problems," Ph.D. thesis, Department of Management Science and Engineering (Operations Research), Stanford University, Palo Alto, CA.
[27] DeMiguel, V., Friedlander, M. P., Nogales, F. J., and Scholtes, S., 2005, "A Two-Sided Relaxation Scheme for Mathematical Programs With Equilibrium Constraints," SIAM J. Optim., **16**(2), pp. 587–609.
[28] Lu, S., Shanbhag, U. V., and Kim, H. M., 2008, "Multidisciplinary and Multilevel Design Optimization Problems With Complementarity Constraints," Proceedings of the 12th AIAA/ISSMO Multidisciplinary Analysis and Optimization Conference.
[29] Wichert, B., 1997, "PV-Diesel Hybrid Energy Systems for Remote Area Power Generation—A Review of Current Practice and Future Developments," Renewable Sustainable Energy Rev., **1**, pp. 209–228.
[30] Diaf, S., Notton, G., Belhamel, M., Haddadi, M., and Louche, A., 2008, "Design and Techno-Economical Optimization for Hybrid PV/Wind System Under Various Meteorological Conditions," Appl. Energy, **85**, pp. 968–987.
[31] Yang, H., Lu, L., and Zhou, W., 2007, "A Novel Optimization Sizing Model for Hybrid Solar-Wind Power Generation System," Sol. Energy, **81**(1), pp. 76–84.
[32] Alhusein, M., Abu-Leiyah, O., and Inayatullah, G., 1993, "A Combined System of Renewable Energy for Grid-Connected Advanced Communities," Renewable Energy, **3**(6–7), pp. 563–566.
[33] Billinton, R., and Chen, H., 1999, "Determination of the Optimum Site-Matching Wind Turbine Using Risk-Based Capacity Benefit Factors," IEE Proc.: Gener. Transm. Distrib., **146**(1), pp. 96–102.
[34] Chaurey, A., and Deambi, S., 1992, "Battery Storage for PV Power Systems: An Overview," Renewable Energy, **2**(3), pp. 227–235.
[35] Ai, B., Yang, H., Shen, H., and Liao, X., 2003, "Computer-Aided Design of PV/Wind Hybrid System," Renewable Energy, **28**(10), pp. 1491–1512.
[36] Groumpos, P., and Papageorgiou, G., 1987, "An Optimal Sizing Method for Stand-Alone Photovoltaic Power Systems," Sol. Energy, **38**(5), pp. 341–351.
[37] Lazou, A. A., and Papatsoris, A. D., 2000, "The Economics of Photovoltaic Stand-Alone Residential Households: A Case Study for Various European and Mediterranean Locations," Sol. Energy Mater. Sol. Cells, **62**(4), pp. 411–427.
[38] Baumrucker, B. T., Renfrob, J. G., and Bieglera, L., 2008, "MPEC Problem Formulations and Solution Strategies With Chemical Engineering Applications," Comput. Chem. Eng., **32**, pp. 2903–2913.
[39] Hobbs, B. F., and Pang, J. S., 2007, "Nash-Cournot Equilibria in Electric Power Markets With Piecewise Linear Demand Functions and Joint Constraints," Oper. Res., **55**(1), pp. 113–127.
[40] Sobieszczanski-Sobieski, J., 1995, *Multidisciplinary Design Optimization: An Emerging New Engineering Discipline*, Advances in Structural Optimization, Kluwer Academic, The Netherlands, pp. 483–496.
[41] Bertsekas, D. P., 2003, *Nonlinear Programming*, 2nd ed., Athena Scientific, Belmont, MA.
[42] Bertsekas, D. P., Nedić, A., and Ozdaglar, A. E., 2003, *Convex Analysis and Optimization*, Athena Scientific, Belmont, MA.

[43] Tosserams, S., Etman, L. F. P., Papalambros, P. Y., and Rooda, J. E., 2006, "An Augmented Lagrangian Relaxation for Analytical Target Cascading Using the Alternating Direction Method of Multipliers," Struct. Multidiscip. Optim., **31**(3), p. 176–189.
[44] Diaf, S., Belhamel, M., Haddadi, M., and Louche, A., 2008, "Technical and Economic Assessment of Hybrid Photovoltaic/Wind System With Battery Storage in Corsica Island," Energy Policy, **36**(2), pp. 743–754.
[45] Diaf, S., Diaf, D., Belhamel, M., Haddadi, M., and Louche, A., 2007, "A Methodology for Optimal Sizing of Autonomous Hybrid PV/Wind System," Energy Policy, **35**(11), pp. 5708–5718.
[46] 2010, https://analysis.nrel.gov/homer/, accessed in February.
[47] 2010, http://www.solarbuzz.com, accessed in February.